Electronic Supplementary Information for:

Selective fluorescent sensing and photocatalytic properties of three MOFs based on naphthalene-1,4-dicarboxylic acid and 2,4,5-tri(4-pyridyl)-imidazole

Jun-Jie Wang,[a,*] Ren-Chun Zhang,[a] Ya-Li Cao,[a] Yan-Ang Li,[a] Yi-Ran Wang[a] and Qing-Lun Wang [b,*]

[a]*College of Chemistry and Chemical Engineering, and Henan Key Laboratory of New Optoelectric Functional Materials, Anyang Normol University, Anyang, Henan, 455000, P. R. China. E-mail: jjwang@aynu.edu.cn*

[b]*College of Chemistry, Nankai University, Tianjin, 300071, P. R. China. E-mail: wangql@nankai.edu.cn*

Table S1. Selected bond distances (Å) and angles (deg) for compounds **1**–**3**.

		1	
Mn(1)-O(3)	2.150(2)	Mn(1)-O(1)	2.151(2)
Mn(1)-N(1)	2.280(3)	Mn(1)-N(7)#1	2.283(3)
Mn(1)-N(2)#2	2.298(3)	Mn(1)-N(6)	2.303(3)
O(3)-Mn(1)-O(1)	171.07(9)	O(3)-Mn(1)-N(1)	89.76(10)
O(1)-Mn(1)-N(1)	81.47(10)	O(3)-Mn(1)-N(7)#1	91.63(10)
O(1)-Mn(1)-N(7)#1	86.96(11)	N(1)-Mn(1)-N(7)#1	91.44(10)
O(3)-Mn(1)-N(2)#2	91.98(10)	O(1)-Mn(1)-N(2)#2	89.71(10)
N(1)-Mn(1)-N(2)#2	90.05(10)	N(7)#1-Mn(1)-N(2)#2	176.11(10)
O(3)-Mn(1)-N(6)	87.45(10)	O(1)-Mn(1)-N(6)	101.37(10)
N(1)-Mn(1)-N(6)	176.68(10)	N(7)#1-Mn(1)-N(6)	90.45(10)
N(2)#2-Mn(1)-N(6)	88.24(10)		
		2	
Zn(3)-O(6)#6	1.959(3)	Zn(3)-O(1)#7	1.962(10)
Zn(3)-O(2')#7	1.962(13)	Zn(3)-N(8)#8	2.054(3)
Zn(4)-O(9)#9	1.950(3)	Zn(4)-O(14)#10	1.972(3)
Zn(4)-N(7)#8	2.029(3)		
O(3)-Zn(1)-O(8)	90.29(13)	O(3)-Zn(1)-N(1)	101.29(13)
O(8)-Zn(1)-N(1)	101.14(13)	O(3)-Zn(1)-O(15)	88.63(13)
O(8)-Zn(1)-O(15)	160.09(12)	N(1)-Zn(1)-O(15)	98.57(13)
O(3)-Zn(1)-O(12)	160.00(12)	O(8)-Zn(1)-O(12)	87.78(13)
N(1)-Zn(1)-O(12)	98.61(12)	O(15)-Zn(1)-O(12)	86.48(12)
O(16)-Zn(2)-N(6)	102.22(13)	O(16)-Zn(2)-O(11)	89.56(14)
N(6)-Zn(2)-O(11)	101.42(12)	O(16)-Zn(2)-O(7)	158.46(12)
N(6)-Zn(2)-O(7)	99.30(14)	O(11)-Zn(2)-O(7)	87.03(14)
O(16)-Zn(2)-O(4)	88.23(14)	N(6)-Zn(2)-O(4)	99.59(13)
O(11)-Zn(2)-O(4)	158.86(12)	O(7)-Zn(2)-O(4)	87.35(14)
O(6)#6-Zn(3)-O(1)#7	90.0(2)	O(6)#6-Zn(3)-O(2')#7	112.9(4)
O(1)#7-Zn(3)-O(2')#7	29.0(3)	O(6)#6-Zn(3)-N(3)	116.68(13)

O(1)#7-Zn(3)-N(3)	120.6(3)	O(2')#7-Zn(3)-N(3)	118.9(4)
O(6)#6-Zn(3)-N(8)#8	111.45(14)	O(1)#7-Zn(3)-N(8)#8	114.1(3)
O(2')#7-Zn(3)-N(8)#8	88.5(3)	N(3)-Zn(3)-N(8)#8	103.97(13)
O(9)#9-Zn(4)-O(14)#10	97.03(14)	O(9)#9-Zn(4)-N(7)#8	114.07(14)
O(14)#10-Zn(4)-N(7)#8	114.30(14)	O(9)#9-Zn(4)-N(2)	110.57(13)
O(14)#10-Zn(4)-N(2)	114.53(15)	N(7)#8-Zn(4)-N(2)	106.39(12)

3

Cd(1)-O(1)	2.233(2)	Cd(1)-O(5)	2.286(3)
Cd(1)-N(1)	2.299(3)	Cd(1)-O(16)#1	2.327(2)
Cd(1)-O(17)	2.363(3)	Cd(1)-N(10)#2	2.386(2)
Cd(2)-O(2)	2.262(2)	Cd(2)-O(10)	2.297(4)
Cd(2)-O(6)	2.325(2)	Cd(2)-N(5)#3	2.339(3)
Cd(2)-O(15)#1	2.372(2)	Cd(2)-O(9)	2.423(3)
Cd(2)-O(16)#1	2.506(2)	Cd(3)-O(3)	2.262(2)
Cd(3)-O(13)	2.298(2)	Cd(3)-O(8)#4	2.334(3)
Cd(3)-O(11)#5	2.349(4)	Cd(3)-N(9)#6	2.370(3)
Cd(3)-O(12)#5	2.399(3)	Cd(3)-O(7)#4	2.603(2)
Cd(4)-O(4)	2.220(2)	Cd(4)-O(14)	2.258(3)
Cd(4)-N(6)	2.317(3)	Cd(4)-O(7)#4	2.324(2)
Cd(4)-O(18)	2.357(3)	Cd(4)-N(4)#7	2.374(2)

O(1)-Cd(1)-O(5)	92.86(12)	O(1)-Cd(1)-N(1)	175.21(10)
O(5)-Cd(1)-N(1)	91.58(12)	O(1)-Cd(1)-O(16)#1	89.16(9)
O(5)-Cd(1)-O(16)#1	112.53(9)	N(1)-Cd(1)-O(16)#1	87.48(9)
O(1)-Cd(1)-O(17)	93.33(11)	O(5)-Cd(1)-O(17)	161.43(12)
N(1)-Cd(1)-O(17)	82.98(11)	O(16)#1-Cd(1)-O(17)	85.05(9)
O(1)-Cd(1)-N(10)#2	86.59(10)	O(5)-Cd(1)-N(10)#2	80.01(11)
N(1)-Cd(1)-N(10)#2	95.95(10)	O(16)#1-Cd(1)-N(10)#2	166.97(9)
O(17)-Cd(1)-N(10)#2	82.90(11)	O(2)-Cd(2)-O(10)	95.20(16)
O(2)-Cd(2)-O(6)	89.07(10)	O(10)-Cd(2)-O(6)	88.31(13)
O(2)-Cd(2)-N(5)#3	172.22(11)	O(10)-Cd(2)-N(5)#3	91.90(17)
O(6)-Cd(2)-N(5)#3	87.96(10)	O(2)-Cd(2)-O(15)#1	89.40(11)

O(10)-Cd(2)-O(15)#1	141.29(13)	O(6)-Cd(2)-O(15)#1	130.26(9)
N(5)#3-Cd(2)-O(15)#1	87.04(12)	O(2)-Cd(2)-O(9)	97.05(12)
O(10)-Cd(2)-O(9)	53.76(14)	O(6)-Cd(2)-O(9)	141.90(11)
N(5)#3-Cd(2)-O(9)	89.71(12)	O(15)#1-Cd(2)-O(9)	87.53(11)
O(2)-Cd(2)-O(16)#1	92.40(9)	O(10)-Cd(2)-O(16)#1	163.35(14)
O(6)-Cd(2)-O(16)#1	77.01(8)	N(5)#3-Cd(2)-O(16)#1	79.92(9)
O(15)#1-Cd(2)-O(16)#1	53.40(8)	O(9)-Cd(2)-O(16)#1	139.72(10)
O(3)-Cd(3)-O(13)	91.48(10)	O(3)-Cd(3)-O(8)#4	87.78(10)
O(13)-Cd(3)-O(8)#4	129.77(10)	O(3)-Cd(3)-O(11)#5	99.19(15)
O(13)-Cd(3)-O(11)#5	88.84(12)	O(8)#4-Cd(3)-O(11)#5	140.78(12)
O(3)-Cd(3)-N(9)#6	170.20(11)	O(13)-Cd(3)-N(9)#6	91.15(10)
O(8)#4-Cd(3)-N(9)#6	83.28(11)	O(11)#5-Cd(3)-N(9)#6	90.30(15)
O(3)-Cd(3)-O(12)#5	95.61(10)	O(13)-Cd(3)-O(12)#5	142.46(10)
O(8)#4-Cd(3)-O(12)#5	87.40(10)	O(11)#5-Cd(3)-O(12)#5	53.64(13)
N(9)#6-Cd(3)-O(12)#5	88.03(11)	O(3)-Cd(3)-O(7)#4	91.22(8)
O(13)-Cd(3)-O(7)#4	77.14(8)	O(8)#4-Cd(3)-O(7)#4	52.69(8)
O(11)#5-Cd(3)-O(7)#4	162.78(14)	N(9)#6-Cd(3)-O(7)#4	80.17(9)
O(12)#5-Cd(3)-O(7)#4	139.23(9)	O(4)-Cd(4)-O(14)	93.77(13)
O(4)-Cd(4)-N(6)	171.28(11)	O(14)-Cd(4)-N(6)	94.94(12)
O(4)-Cd(4)-O(7)#4	90.46(9)	O(14)-Cd(4)-O(7)#4	110.95(10)
N(6)-Cd(4)-O(7)#4	86.02(8)	O(4)-Cd(4)-O(18)	85.49(13)
O(14)-Cd(4)-O(18)	162.07(12)	N(6)-Cd(4)-O(18)	86.36(12)
O(7)#4-Cd(4)-O(18)	86.98(10)	O(4)-Cd(4)-N(4)#7	92.41(10)
O(14)-Cd(4)-N(4)#7	79.98(11)	N(6)-Cd(4)-N(4)#7	89.53(9)
O(7)#4-Cd(4)-N(4)#7	168.49(9)	O(18)-Cd(4)-N(4)#7	82.15(11)

Symmetry codes: For **1**: #1: $x-1, y, z$; #2: $x+1, y, z$; For **2**: #6: $x, y, z-1$; #7: $x+1, y, z-1$; #8: $x+1, y-1, z-1$; #9: $x, y-1, z$; #10: $x+1, y-1, z$; For **3**: #1: $-x+1, -y+1, -z+1$; #2: $x, y+1, z$; #3: $-x+2, -y+2, -z+1$; #4: $-x+1, -y+1, -z$; #5: $x-1, y, z$; #6: $-x, -y, -z$; #7: $x, y-1, z$.

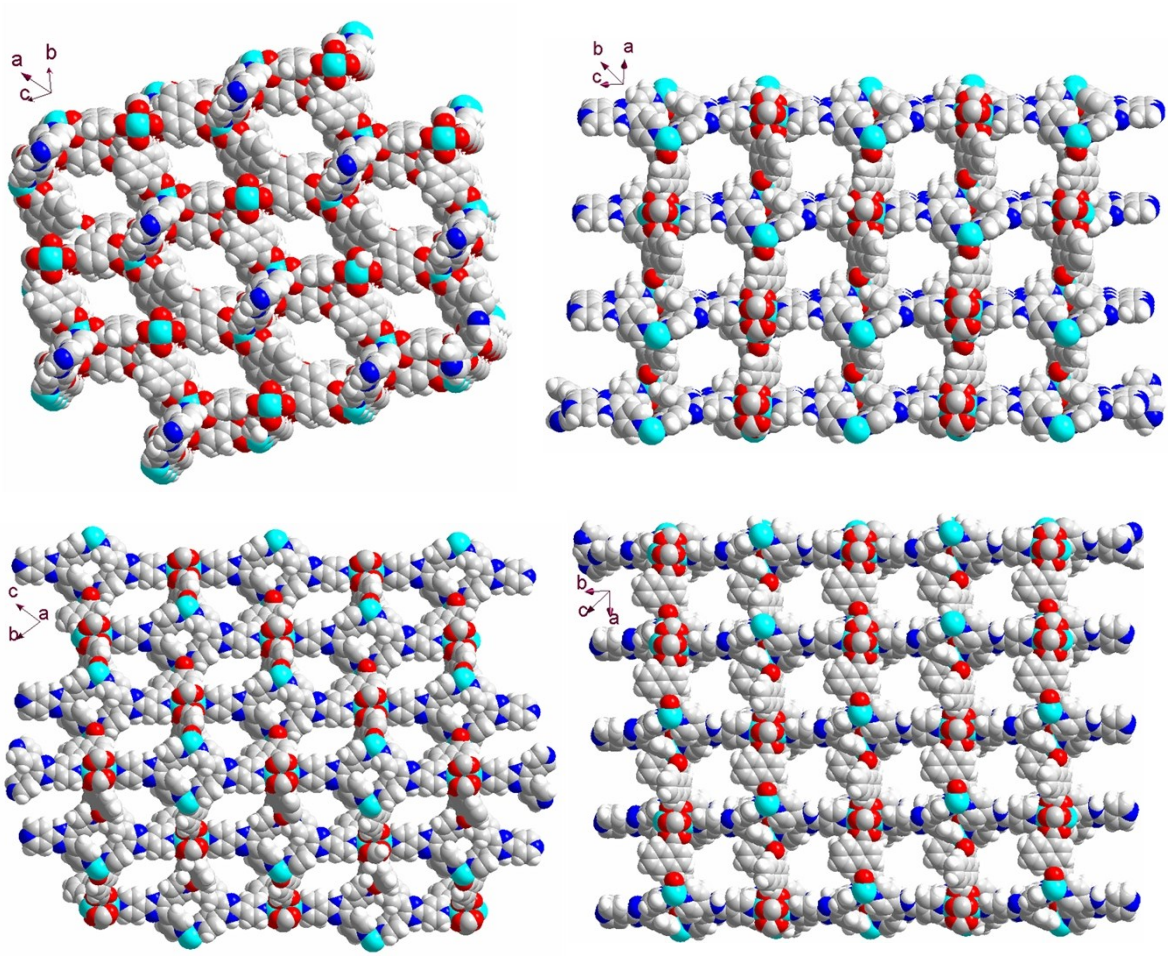

a)

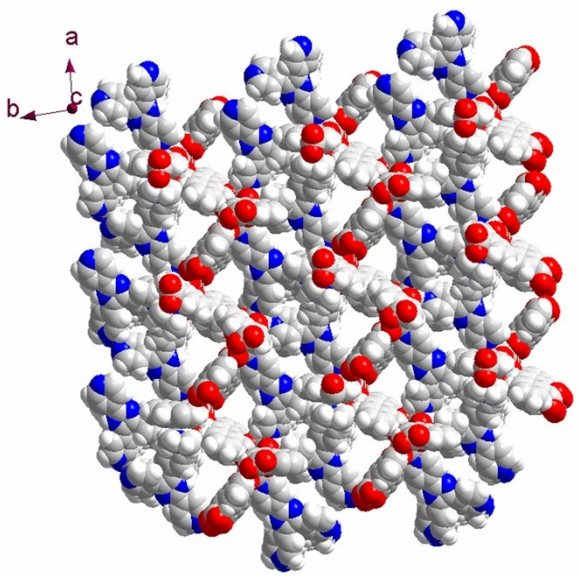

b)

Fig. S1 Perspective View of the channels within compounds **2** (a) and **3**(b), respectively.

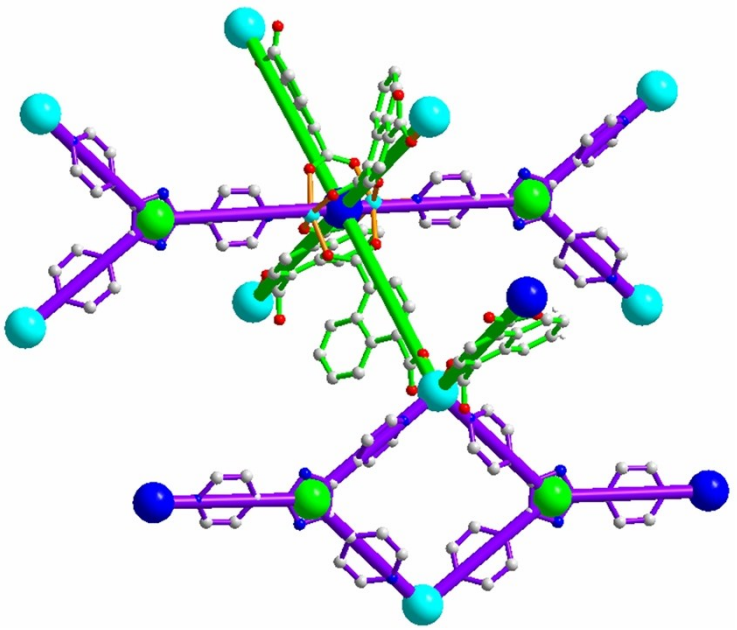

a)

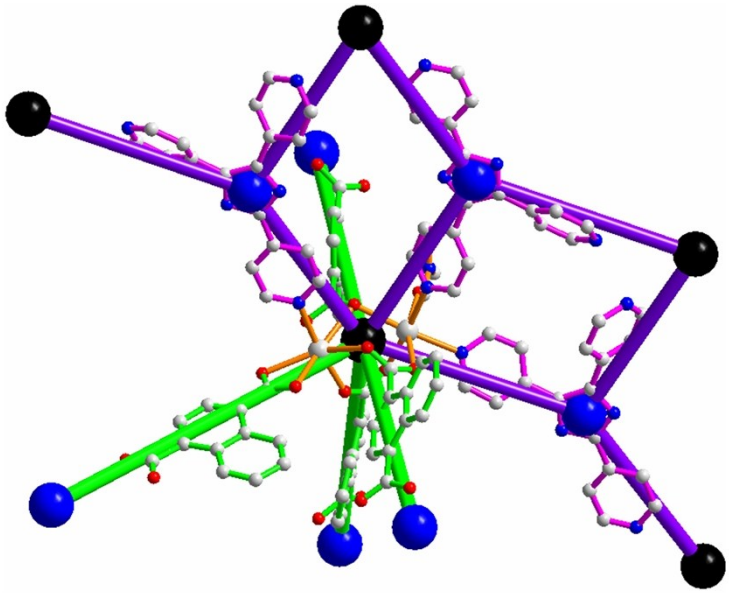

b)

Fig. S2 View of the (3,4,6)-connected nodes and (3,7)-connected nodes in compounds **2** (a) and **3**(b), respectively.

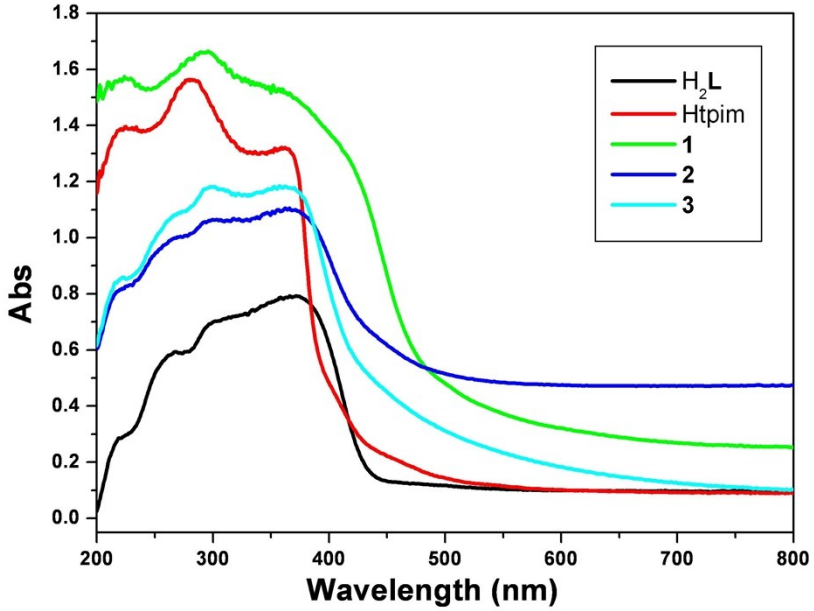

Fig. S3 Solid Uv-Vis absorption spectra for H_2**L** and Htpim and **1–3** at room temperature.

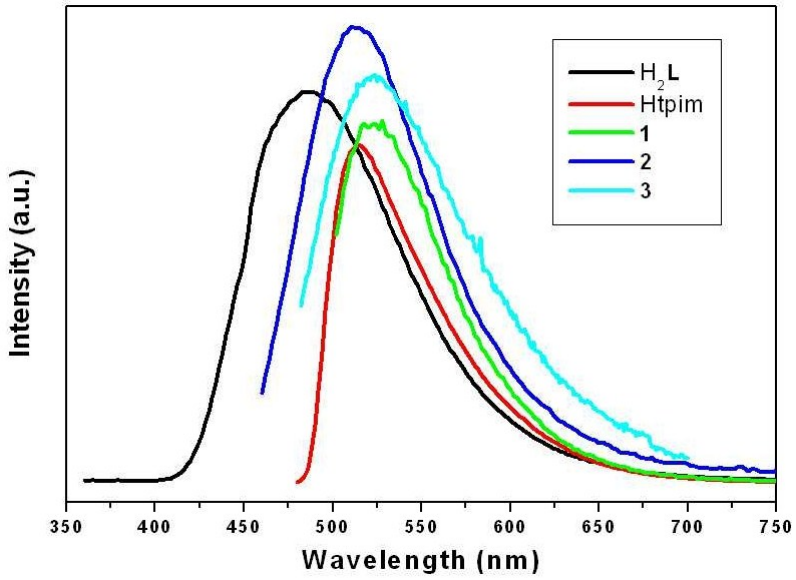

Fig. S4 Emission spectra of H_2**L** and Htpim and **1–3** in the solid state at room temperature (λ_{ex} = 346 nm for H_2**L**, 468 nm for Htpim, 467 nm for **1**, **2** and **3**, respectively).

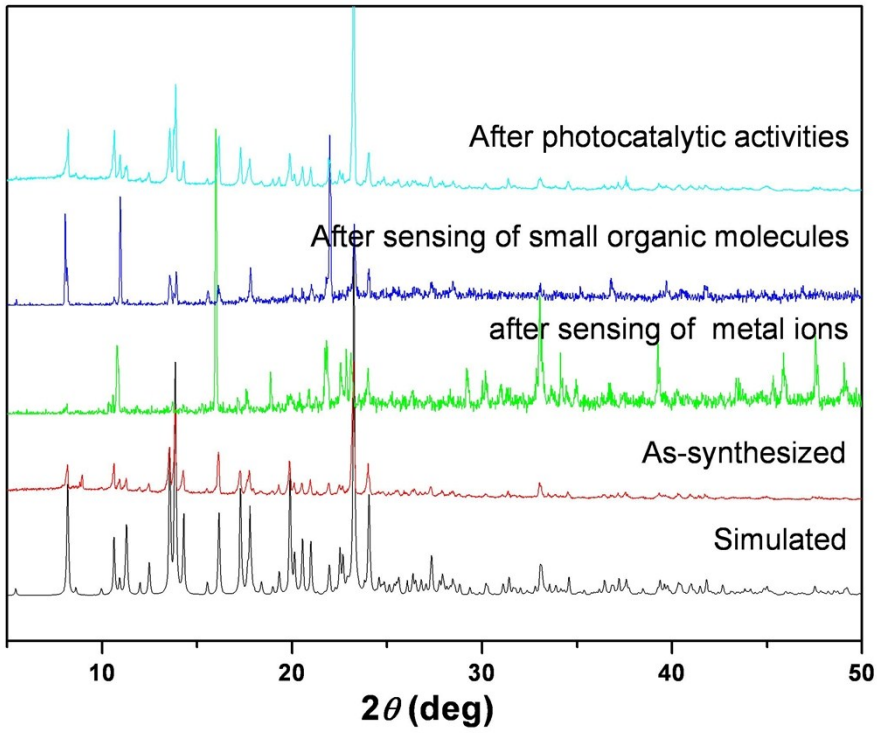
After photocatalytic activities
After sensing of small organic molecules
after sensing of metal ions
As-synthesized
Simulated
10
20
30
40
50
2θ (deg)

a)

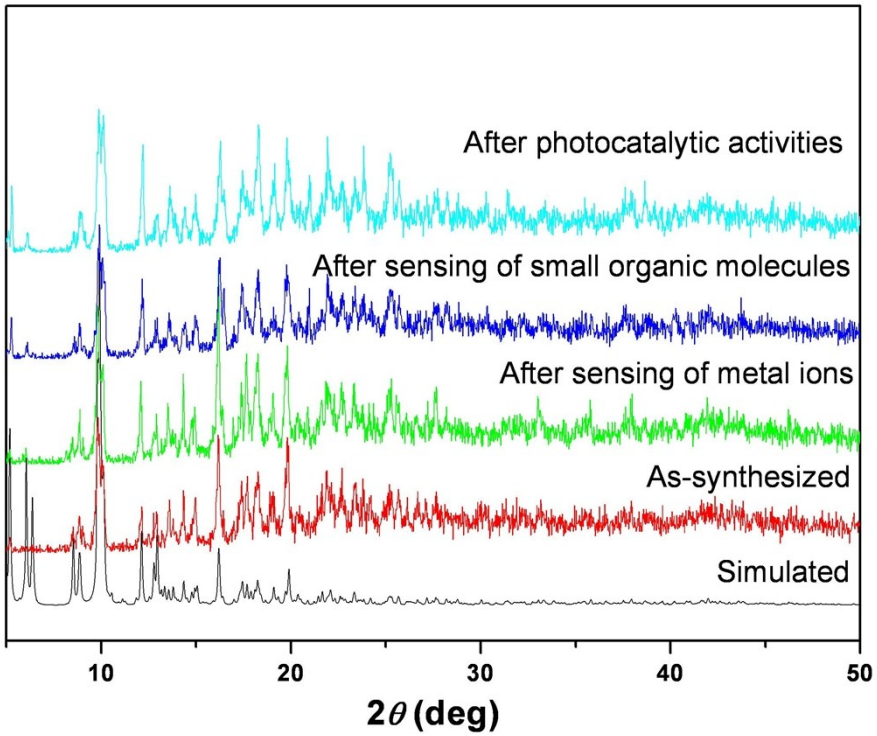
After photocatalytic activities
After sensing of small organic molecules
After sensing of metal ions
As-synthesized
Simulated
10
20
30
40
50
2θ (deg)

b)

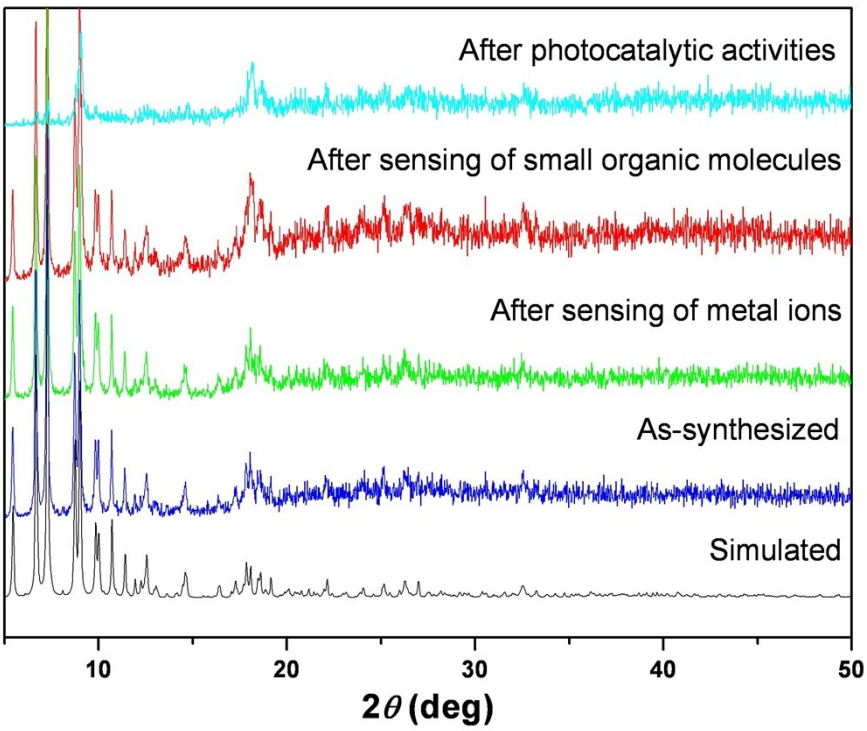

c)

Fig. S5 X-ray powder diffraction (XRPD) patterns of simulated, as-synthesized, after sensing of metal ions and small organic molecules, after photocatalytic activities measured in air, respectively: a) for **1**, b) for **2**, and c) for **3**.

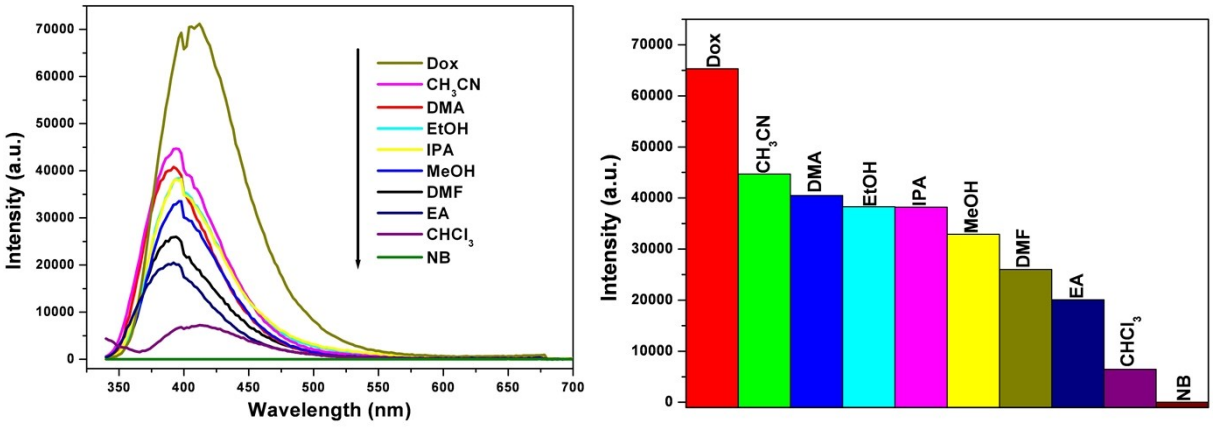

a)

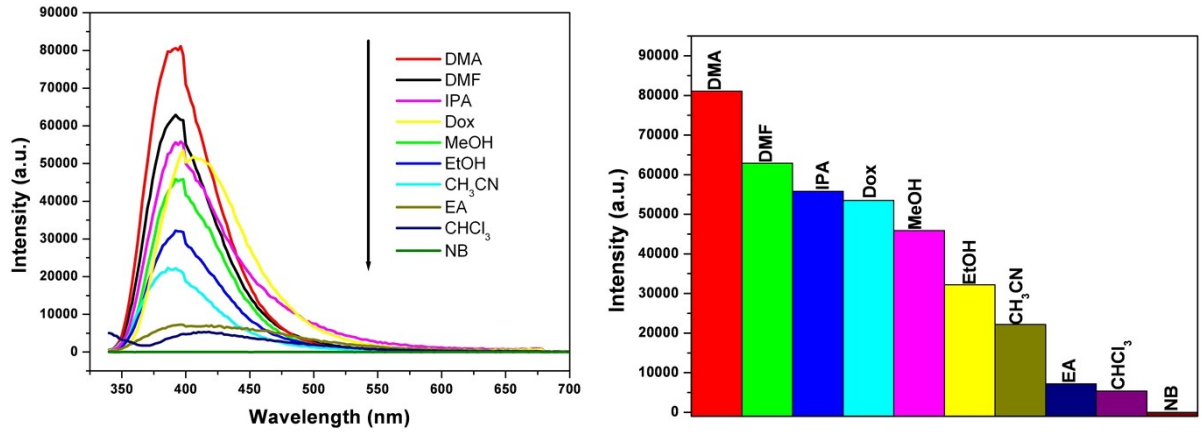

b)

Fig. S6 Emission spectra and intensities for **2** (a) and **3** (b) in different organic solvents.

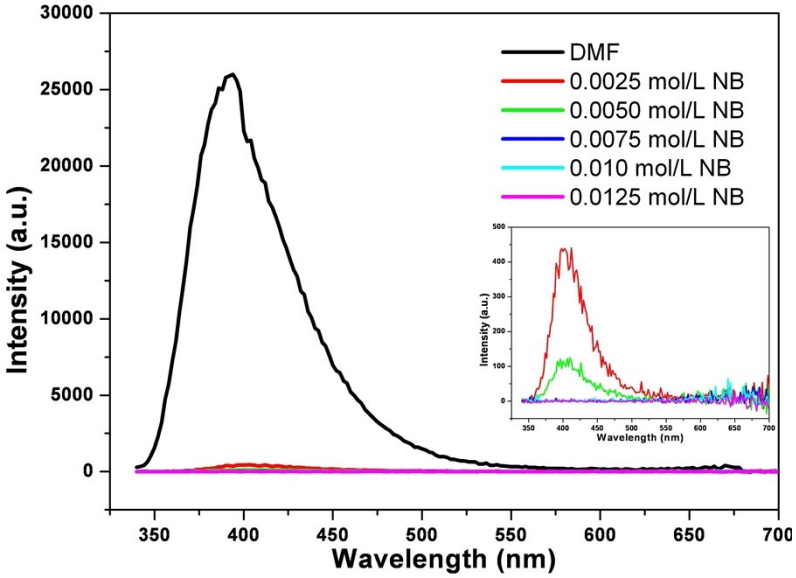

a)

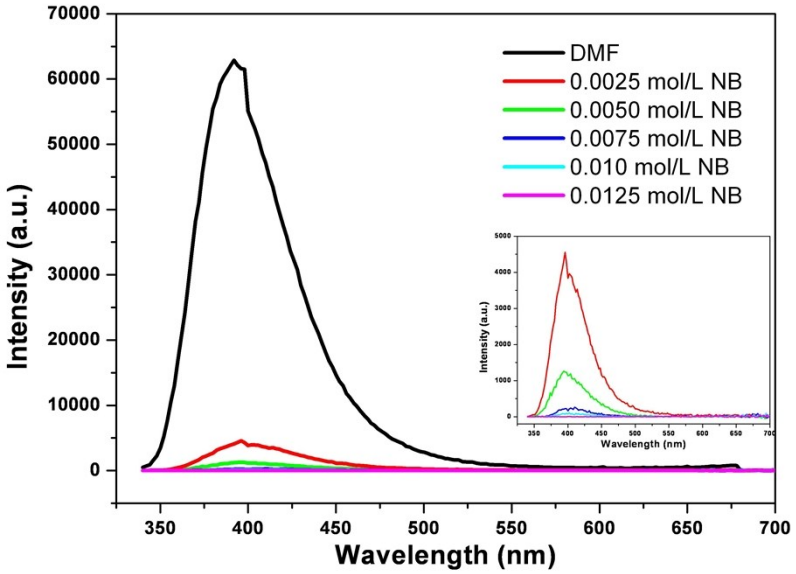

b)

Fig. S7 Emission spectra of compounds **2** (a) and **3** (b) at different NB concentrations in DMF (Inset: Low intensity data of mission spectra of compounds **2** and **3**) (excited at 322nm for **2** and **3**).

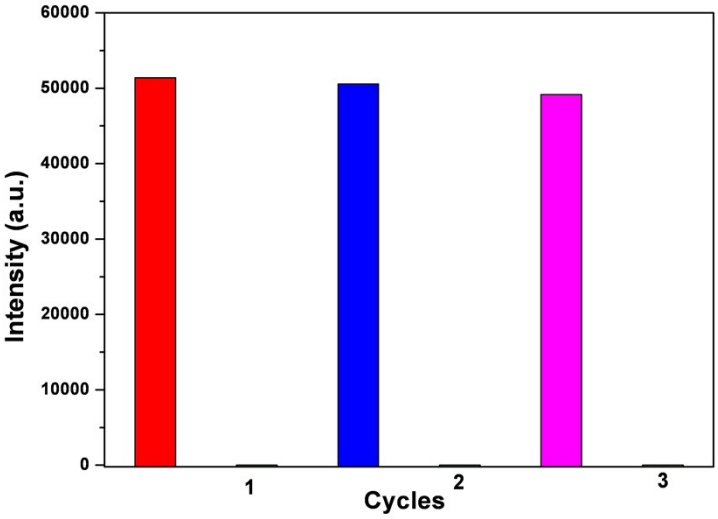

a)

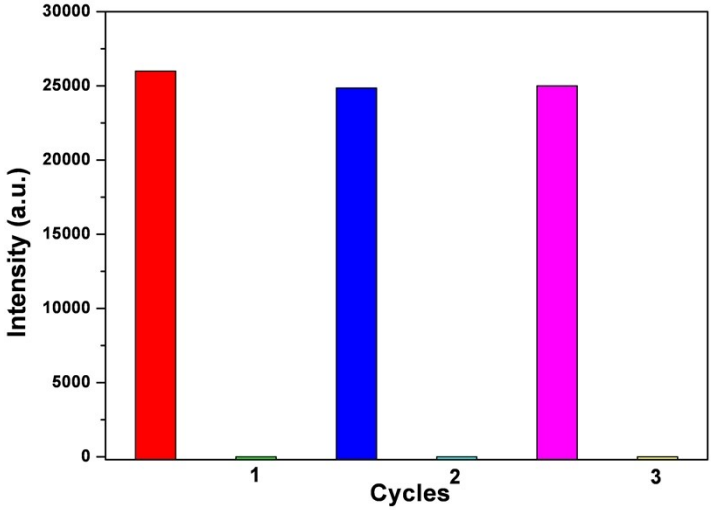

b)

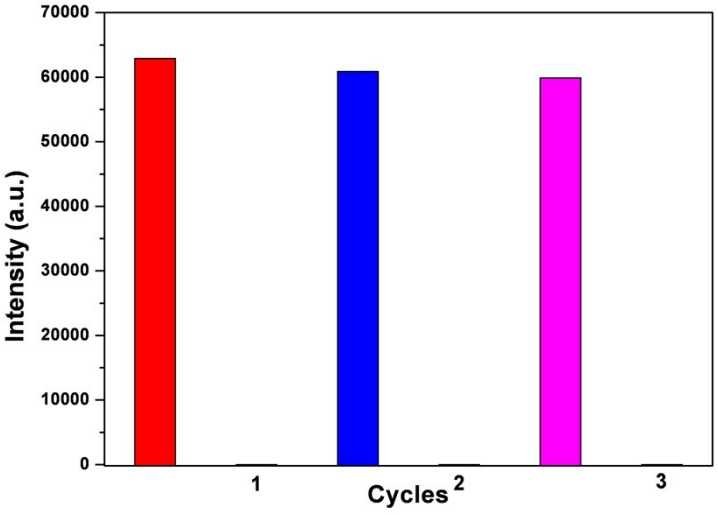

c)

Fig. S8 Recycling test of **1** (a), **2** (b) and **3** (c) as chemical sensors in sensing of nitrobenzene with 3 times.

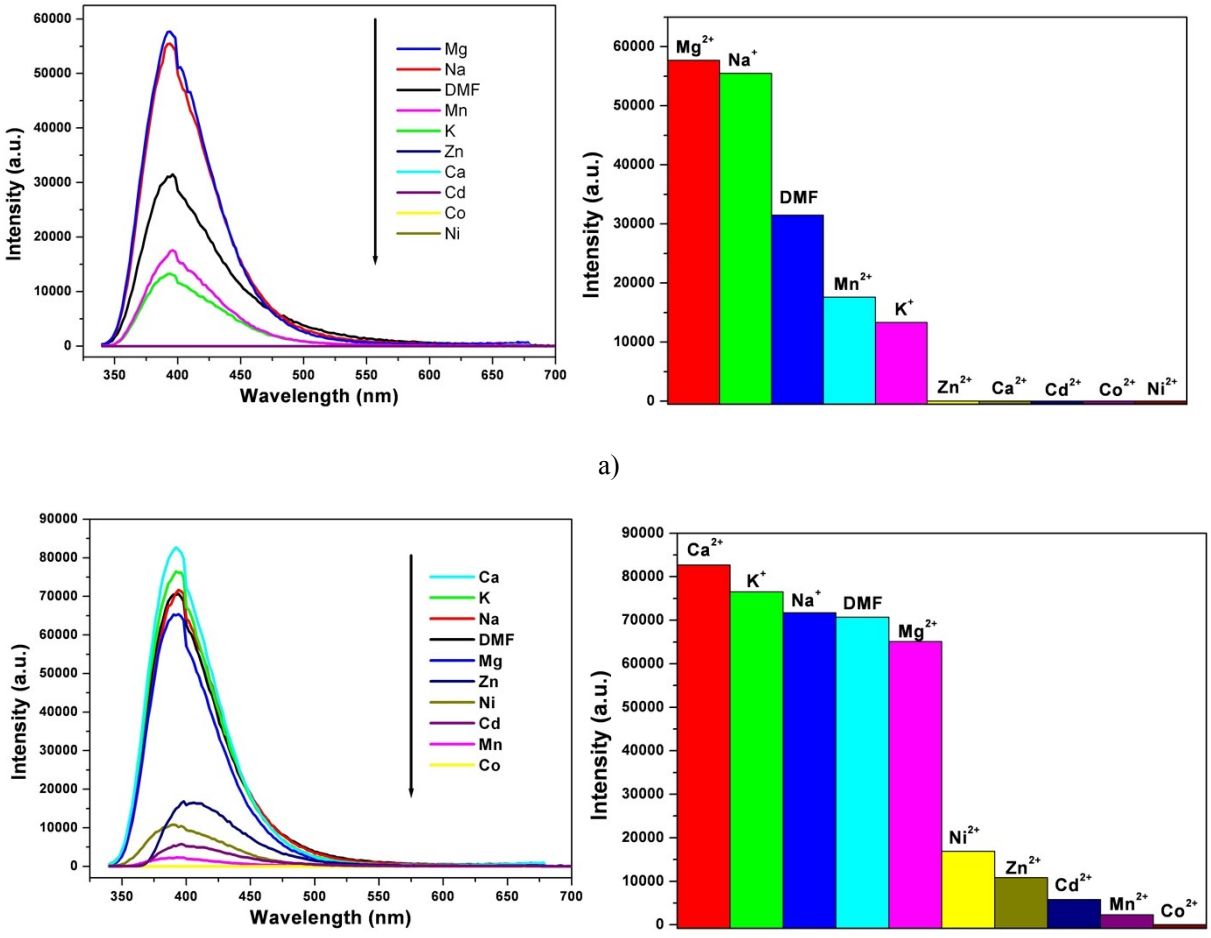

Fig. S9. Emission spectra and intensities for **2** (a) and **3** (b) in DMF solutions of different metal ions.

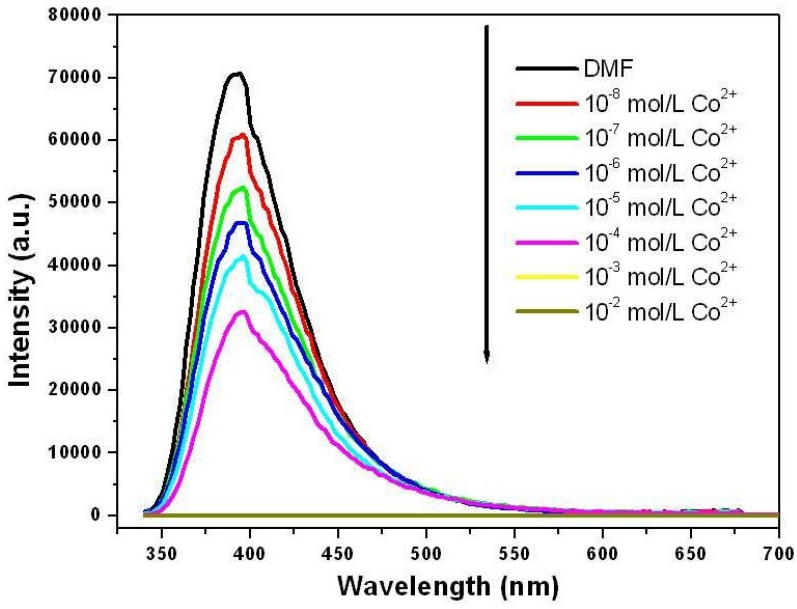

Fig. S10 Emission spectra of compound **3** at different metal ions concentrations in DMF.

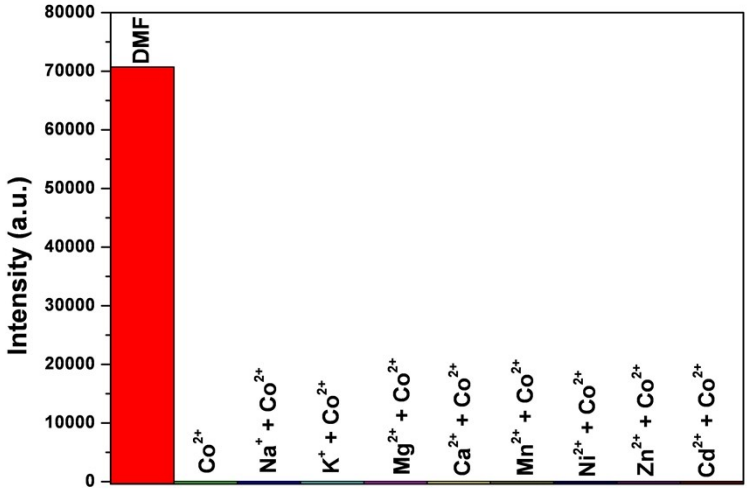

Fig. S11 Emission intensities of **3** in DMF solutions of mixed metal ions (10^{-3} mol/L)..

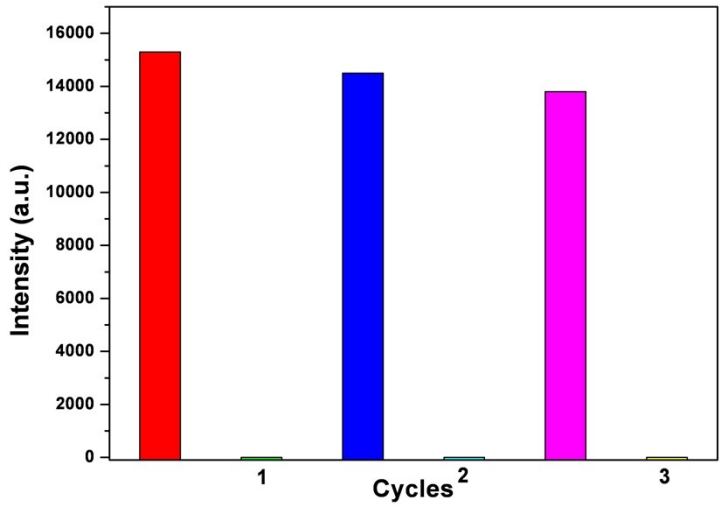

a)

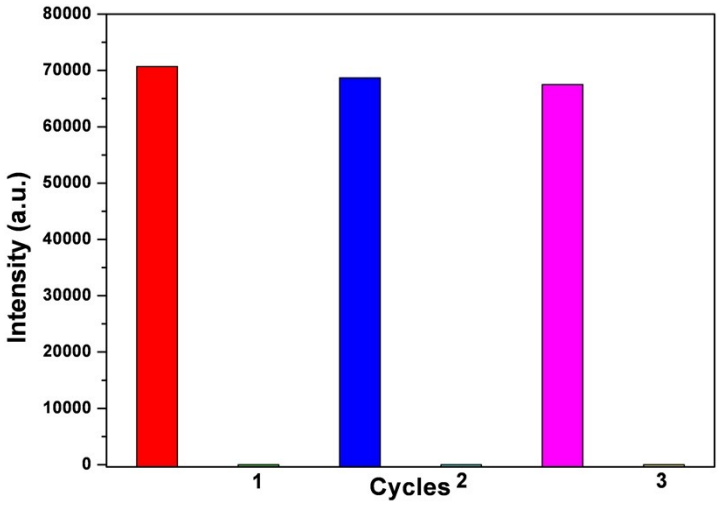

b)

Fig. S12 Recycling test of **1** (a) and **3** (b) as chemical sensors in sensing of metal ions with 3 times.

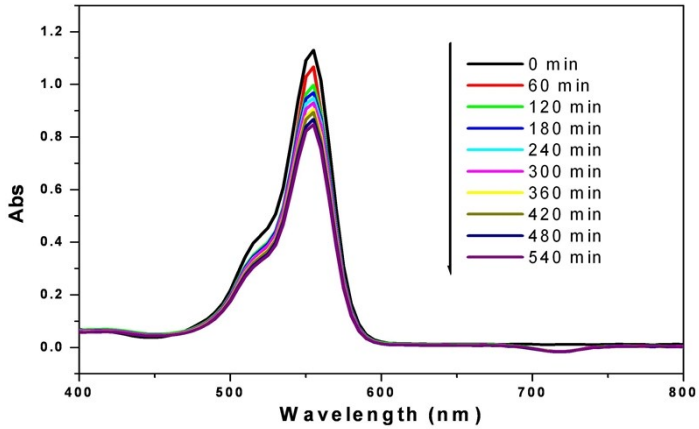
Abs
Wavelength (nm)
0 min
60 min
120 min
180 min
240 min
300 min
360 min
420 min
480 min
540 min

a)

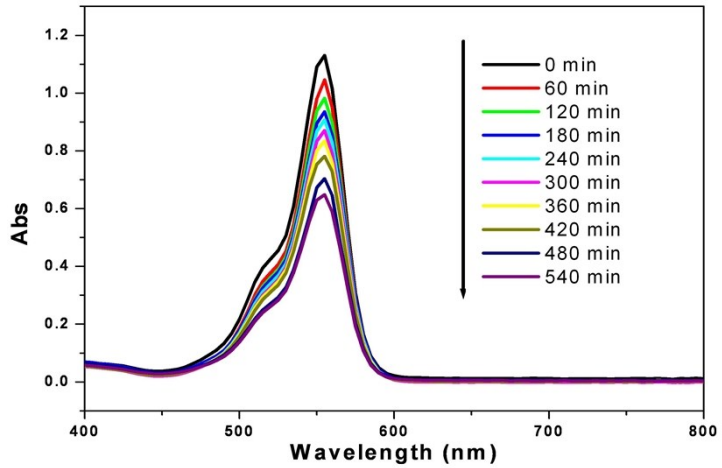
Abs
Wavelength (nm)
0 min
60 min
120 min
180 min
240 min
300 min
360 min
420 min
480 min
540 min

b)

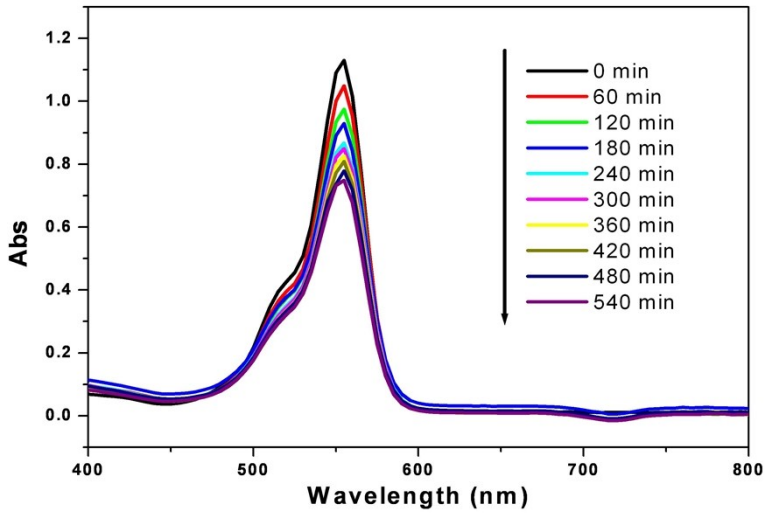
Abs
Wavelength (nm)
0 min
60 min
120 min
180 min
240 min
300 min
360 min
420 min
480 min
540 min

c)

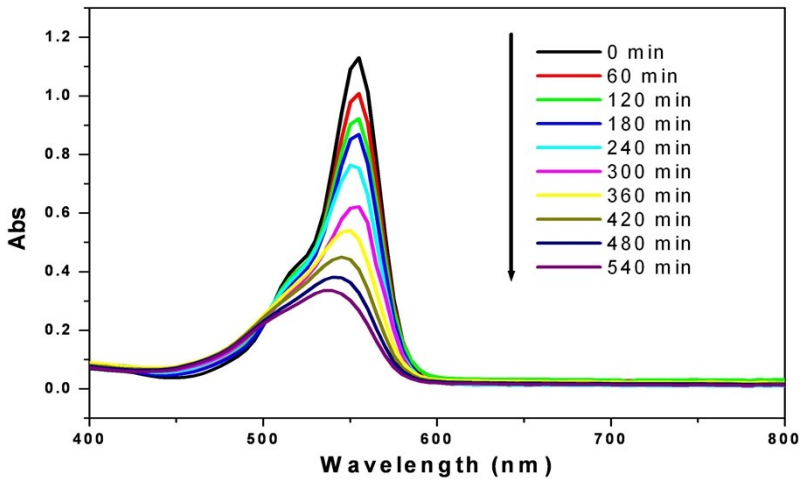

d)

Fig. S13 UV−vis absorption spectra of the RhB solution during the decomposition reaction without any catalyst (a) or in the presence of **1** (b), **2** (c) and **3** (d).

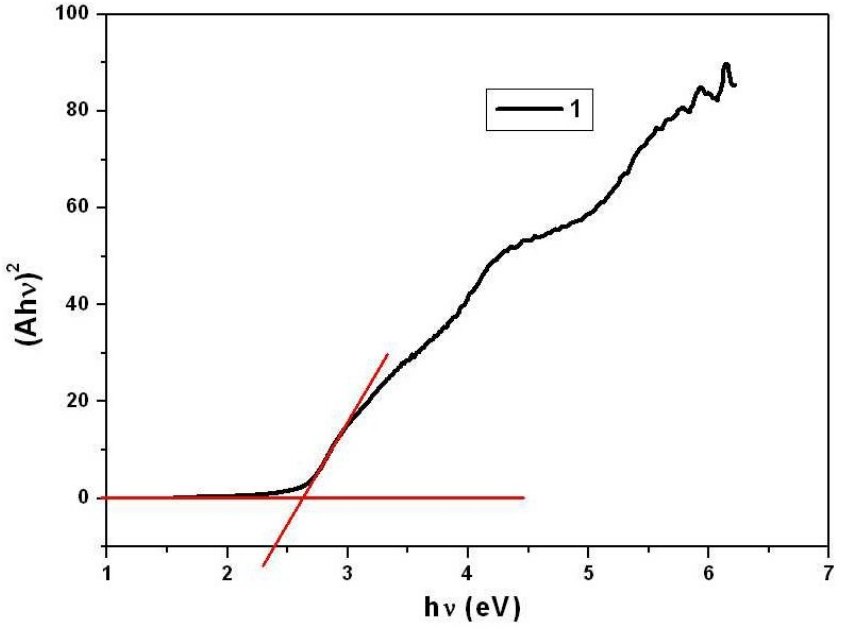

a)

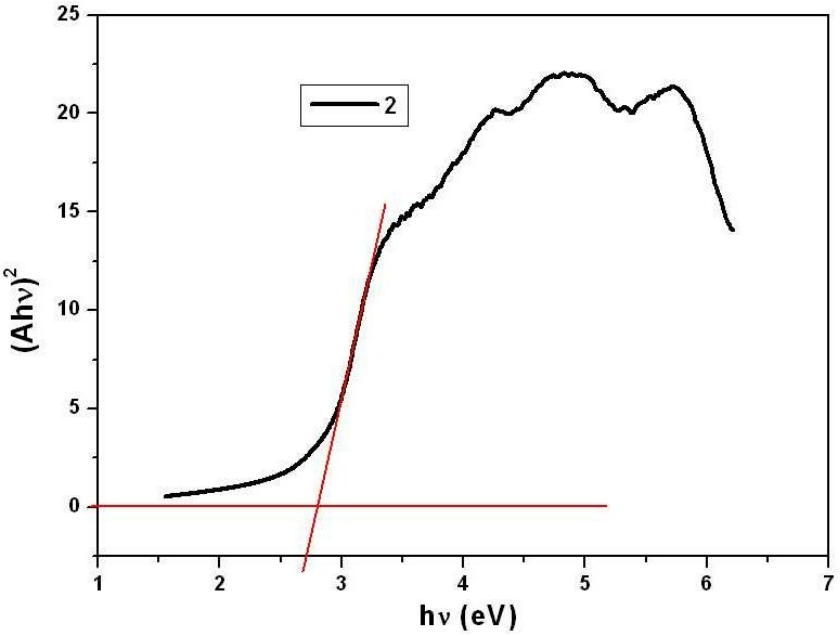

b)

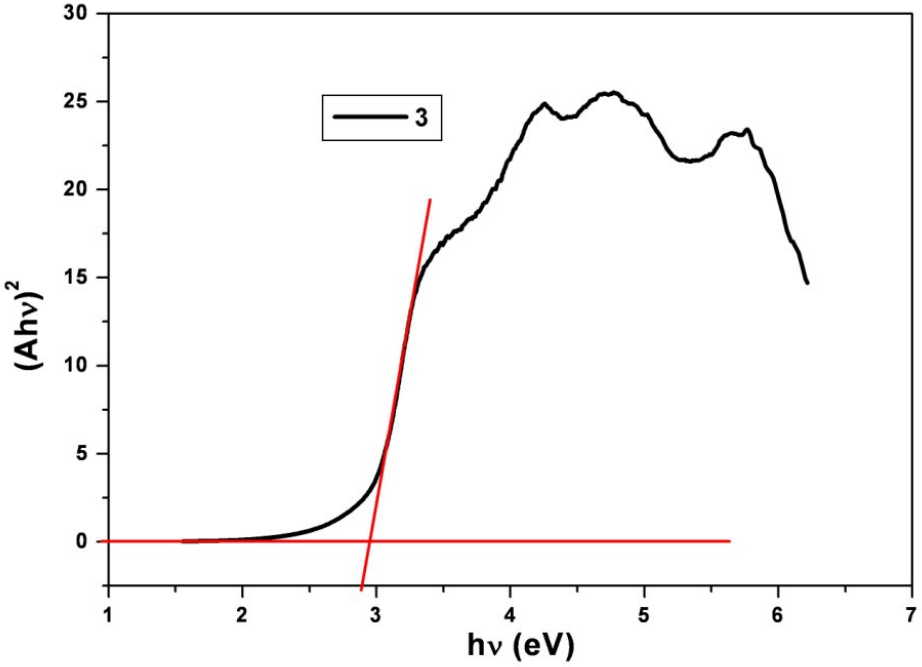

c)

Fig. S14 The $(Ahν)^2$ vs hν curve of **1** (a), **2** (b) and **3** (c).

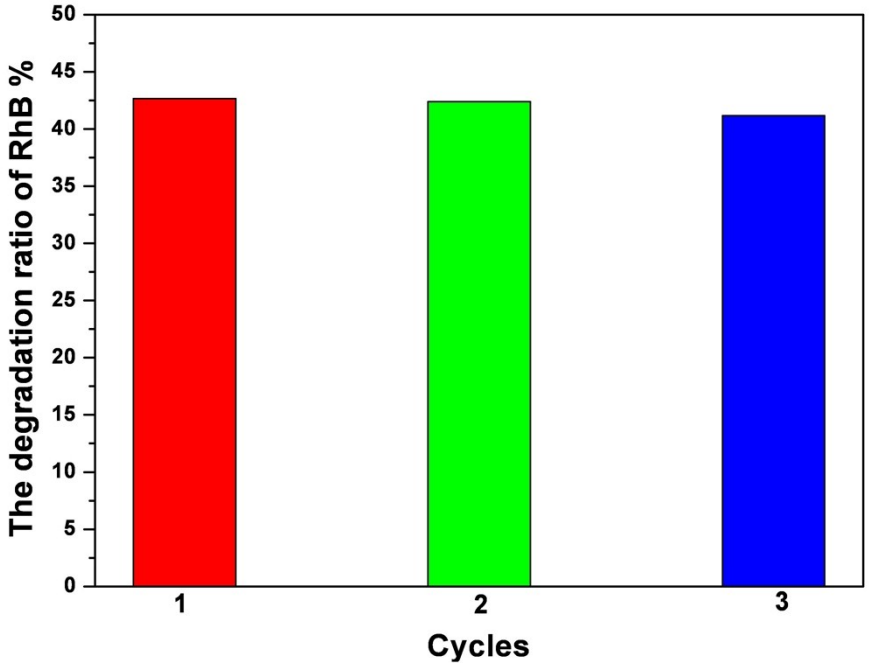

a)

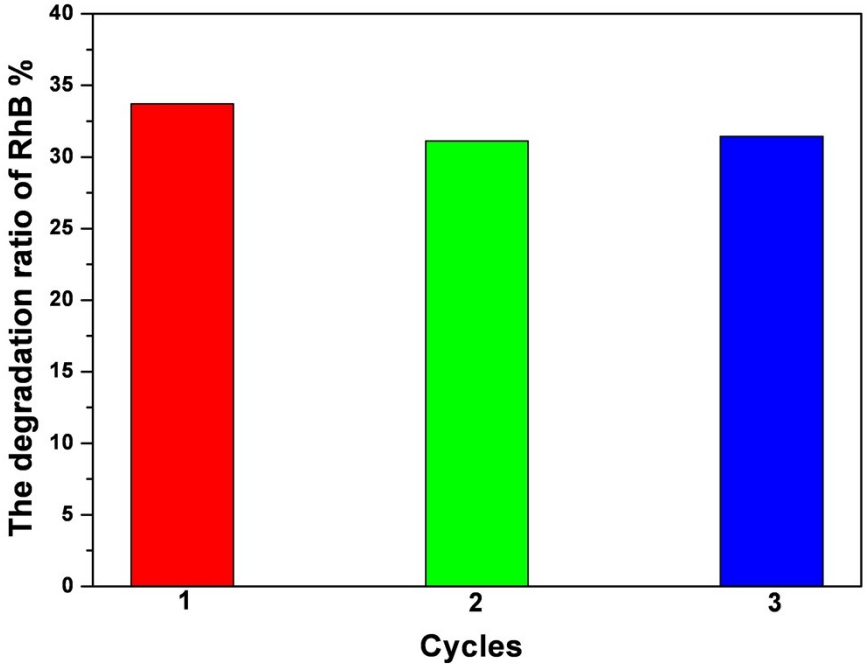

b)

Fig. S15 Recycling test of the photocatalytic degradation of RhB in DMF for **1** (a) and **2** (b) with 3 times.

Thermogravimetric analyses. Thermogravimetric analysis (TGA) experiments were conducted to determine the thermal stabilities of **1**–**3** (Fig. S16). As shown in Fig. S2, the TGA curves of **1** and **2** are similar. The first weight loss occurs in the range of 82-457 °C for **1** and 176-500 °C for **2**, corresponding to the release of one **L** and two Htpim ligands (For **1**, calcd: 53.1%, observed: 55.6%; For **2**, calcd: 52.7%, observed: 53.3%). Then a consecutive weight lose does not end until heating to 800 °C. While in **3**, because of existence of DMF, the framework is only stable up to ca. 71°C. The TGA curve show the first weight loss of two DMF molecules (calcd: 3.8%; observed: 3.6%) occurs in the temperature range of 71–150°C. Secondly, the second weight loss of 10.4% in the range of 150-287°C corresponds to the release of one **L** ligand (calcd: 9.2%). Then, two L ligands and two Htpim ligands (calcd: 48.2%; observed: 50.0%) are released in the range of 287–527°C. Finally, the other weight loss does not end until heating to 800°C.

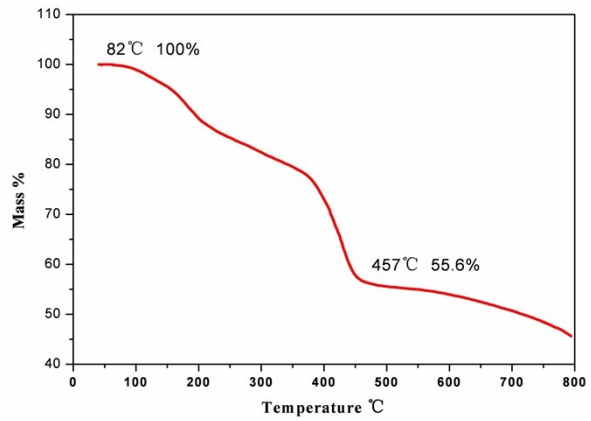

a)

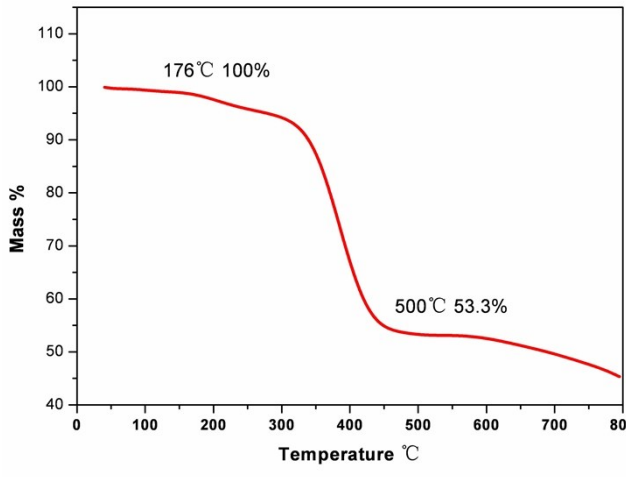

b)

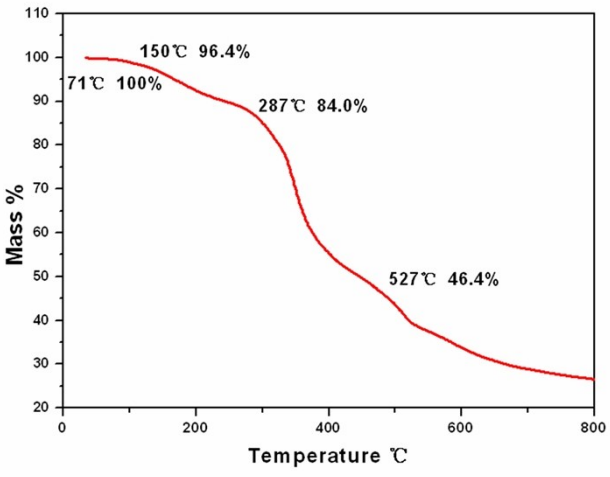

c)

Fig. S16 Thermogravimetric analyses (TG) patterns of a) for **1**, b) for **2** and c) for **3** measured from room temperature to 800 °C, respectively.